



Increase of Charge-Coupled Device Resolution limits using Spatial Light Modulator

Mohammad Sohail*¹, Nigar Fida², Haroon Khan², Muhammad Noman Hayat²

¹Department of Physics, Abdul Wali Khan University, Mardan, KPK, Pakistan
sohail.dagiwal@gmail.com²

²Department of Computer Science, Abdul Wali Khan University, Mardan, KPK, Pakistan
haroon_rajjar@yahoo.com, nigarfida@gmail.com, hayatnoman@gmail.com

ABSTRACT- Resolution of the imaging devices is mainly restricted by the pixels pitch, the pixels size and shape. We show a methodology where a Liquid Crystal on Silicon presentation is utilized to produce diverse direct stages at the article phantom plane, prompting distinctive sub-pixel relocations of the item picture at the picture plane. Along these lines, pictures of the same item with various movements are inspected by Charge-Coupled Device (CCD) camera. At long last, all the acquired pictures are legitimately consolidated prompting a last super-determined picture. Correlation of unique article and the one acquired with our methodology plainly affirm a noteworthy change in determination.

Keywords: Charge Devices, Spatial Light, Resolution

INTRODUCTION

High resolution devices are needed for many purposes such as remote sensing applications or for medical purposes. If the output image taken by imaging device is the same as input object, then we say ideal super-resolution is achieved. In real systems, the resolution of the signal is degraded by many reasons, as for instance, environmental conditions or physical limitations in resolution related to the optical components as well as geometrical components. Gap sizes, flaws and misalignments of optical segments force a determination limits identified with the Point Spread Function (PSF) of the optical framework [1,2]. The complete disposal of these sign debasement is unthinkable however can be minimized to some degree [1-3]. Current imaging frameworks additionally incorporate Charge-Coupled Devices (CCD) that lead to a diminishment in determination created by the geometrical properties of pixel cluster, e.g. pixels shape, pixel size and partition of the pixels cluster (pixel pitch) [3-5]. Resolution of the imaging sensor depends on the density of the sampling points (i.e. the number of the pixels per unit area) and on the pixel size and geometry.

Many approaches have been reported in literature to cover blurring and aliasing problems [4-12], which are originated by these CCD geometric properties. Higher resolution than the provided by the sensor pixel density can be achieved by reconstructing several sub-pixel displaced images. To generate image subpixel displacements, the use of mechanical elements, as mirrors, can be applied [13-14]. Nevertheless, to avoid mechanical errors related to mechanical controlled placements, the use of birefringent materials, as for instance birefringent crystals, can be also applied [15]. However, in such way, only a fixed value for the subpixel displacement can be generated.

In this paper, we present a new experimental approach which helps to improve the resolution limitation imposed by CCD pixels pitch by means different image subpixel displacements generated without the necessity of use any mechanical element in the set-up. To this aim, a reflective Parallel Aligned (PA) Liquid Crystal on Silicon (LCoS) display is used to generate different linear phases at the Fourier spectrum plane of the object. Different encoded linear phases lead to different shifts of the object image at the image plane, where a CCD camera is placed. Controlling the value of the linear phase addressed to the LCoS display, the image is shifted by some fraction of the CCD pixel size, performing subpixel displacements in 2-D of the image object. Finally, all the images are combined leading to a final image with larger dimension than the original object.

I. EXPERIMENTAL SETUP

The set-up used to apply this technique is sketched in Fig. 1. The object scene is illuminated with a coherent laser beam of 633 nm wavelength (He-Ne laser). A Spatial Filter (SF) is placed at the exit of the laser source to reduce the signal to noise ratio and to expand

the light beam. Followed to the SF, a convergent lens is properly placed leading to a collimated illumination at its back. Placed just after it, we have set a Linear Polarizer (LP) with its transmissive axis oriented at 90 degrees of the laboratory vertical (i.e. at the same orientation of liquid crystal molecules extraordinary axis). In this way, the PA LCoS display operates in a phase-only on figuration. Afterwards, the collimated beam exiting from the LP reaches the convergent lens L1, leading to a convergent illumination of object. At the focal plane of the lens L1, the Fourier spectrum of object with a given scaled factor is formed. At this plane, the Parallel Aligned (PA) LCoS display is situated. A Beam Splitter (B-S) is also included in the set-up, to steer the light reflected by the PA LCoS display at the reflected set-up arm.

At this stage, we address different linear phases to the PA LCoS display to encode the object spectrum plane. At the reflected beam, a convergent lens L2 is placed. Then, the encoded object spectrum at the PA LCoS display plane is inverse Fourier transform by L2 which produce the image of the object at the imaging plane. Finally, the resulting image of the object is sampled by the CCD camera with a resolution of $m \times m$ pixels.

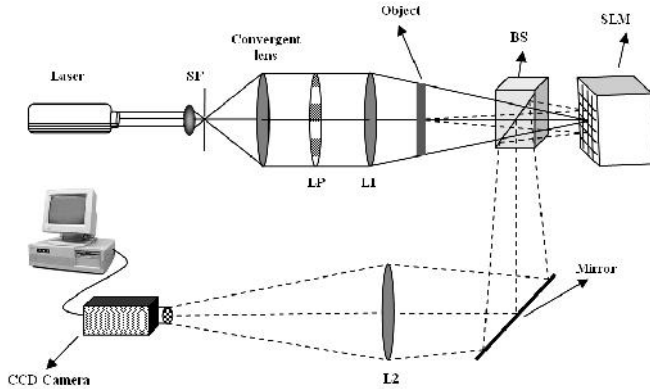


Figure 1. Experimental set-up.

Different linear phases addressed to the PA LCoS display lead to different shifts of the object image at the CCD camera. The system is calibrated to determine the linear phase corresponding to a displacement of 1 pixel at the CCD camera in the x and y directions. By knowing this, it is immediate to determine the linear phase required to produce any displacement of the object image at the CCD camera. In this work, fractions of pixel size (i.e. subpixel displacements) are generated

$$\frac{1}{n_x} \frac{1}{n_y}$$

in 2-D. For every fraction $\frac{1}{n_x} \frac{1}{n_y}$ of the pixel size

selected, $n_x \cdot n_y$ images are recorded to homogenously cover the whole pixel dimension. Finally all the displaced images are properly combined, obtaining the final super-resolved image.

Figure 2 gives a comparison between the original object image (Fig. 2(a)) and the final image obtained when performing our technique with displacements of 1/2 pixel size both in x and y directions (Fig. 2(b)). We obtain a significant improvement in resolution in Fig. 2(b) related to the increase of information provided by different displaced images. This significant improvement is easily observed both in x and y directions (i.e. vertical and horizontal lines in Fig. 2(b)). Smaller displacements (and so, larger dimension images) has been also tested, but the increase of resolution is no so evident when compared with results given in Fig. 2(b). We think that this is because in this situation image resolution is not limited by CCD pixel geometry but by PSF of optical system.

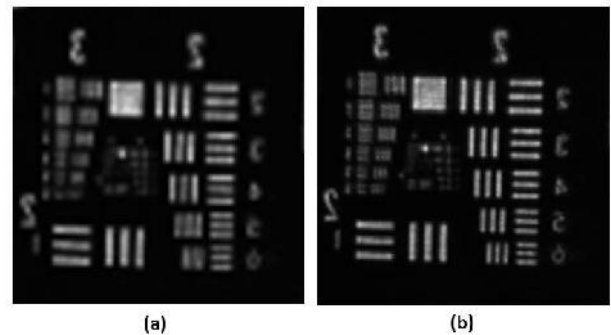


Figure 2. (a) Low resolution image; (b) High resolved image.

Finally, to take into account the blurring effect due to the intensity average performed inside the pixels area, an inverse filtering process [16] in the frequency domain is also applied. Note that the intensity sampled by CCD camera can be described by the convolution of the object image with the square function of the CCD pixel. It is given mathematically as follow,

$$I(x) = o(x) \otimes h(x) \tag{1}$$

being $o(x)$ the object image and $h(x)$ the shape of the CCD pixels that we assume to be squared. The operator \otimes denotes convolution. By applying the Fourier transform to Eq. (1), we obtain

$$\tilde{I}(v) = \tilde{O}(v) \cdot H(v) \tag{2}$$

where $\tilde{O}(v)$ is the Fourier transform of object and $H(v)$ is the sinc(v) function.

Finally, by multiplying each side of Eq. (2) by the conjugate of $H(v)$ and rearranging, we obtained the following relation,

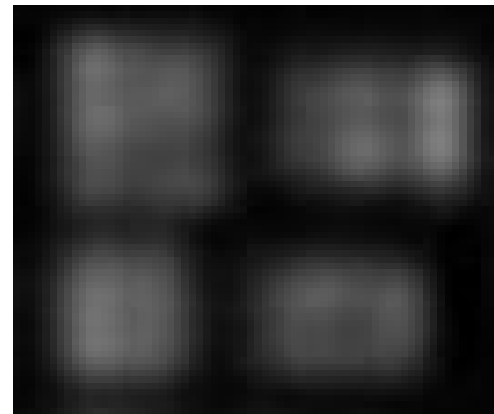
$$O(v) = \frac{\tilde{I}(v) \cdot H^*(v)}{|H(v)|^2 + \dagger} \quad (3)$$

Note that in Eq. (3) we have also included the parameter \dagger . This parameter is imposed to be very small and included to avoid zeros at the denominator of Eq. (3). Finally, by inverse Fourier transforming Eq. (3), a filtered object image (i.e. removed to certain extent of blurring effect) is achieved.

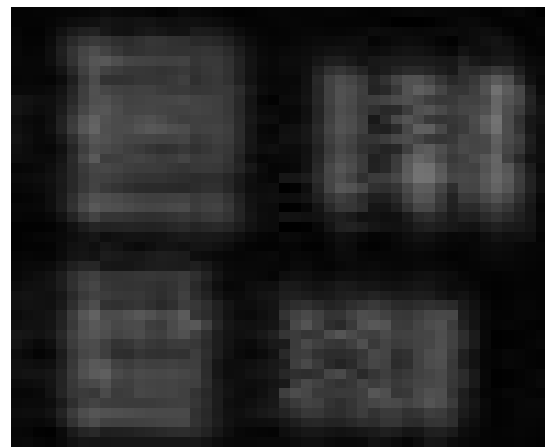
Experimental results are shown in Fig. (3). In order to obtain better insight on the obtained results, the object region showing the limit in resolution of our provided technique (i.e. the higher frequencies in object we are able to resolve) is zoomed. In particular, the object region used to comparison is marked with a dashed circle in Fig. 2(b).

In Fig. 3(a), we show the results for the object region stated before, obtained when the proposed technique is not applied (i.e. low resolution image). We observe that vertical and horizontal lines are not resolved and clearly blurred. The results for the same object region are improved when applying our proposed technique (Fig. 3(b)). Finally, the best results are obtained by combining the filtering process to the images obtained with our approach (Fig. 3(c)). In particular, an object image with more softens edges and reduced of blurring effect is achieved.

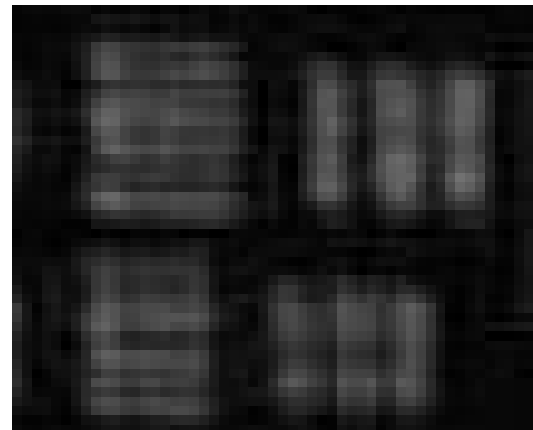
We want to note that results shown in Fig. 3(b) and 3(c) correspond to displacements of 1/4 pixel size both in x and y directions. As stated before, when applying our experimental approach without using the filtering process, a significant improvement of the image resolution is obtained for displacements of 1/2 pixel size. However, by using even smaller displacement values, better results are not obtained. Unlike, when applying the filtering process, the smaller the displacement value, the higher the improvement in resolution achieved. This correlation occurs until certain displacement value (about 1/6 pixel size), where the PSF of the system becomes the main limit in resolution.



(a)



(b)



(c)

Figure. 3. a) Low resolution image; (b) image with high resolution; (c) image obtained using filtration and with high resolution.

II. CONCLUSION

Summarizing, an experimental approach valid to improve resolution limitations imposed by the pixel pitch in CCD cameras is proposed in this paper. This

technique, which does not require any mechanical element, is based on a PA LCoS display. The PA LCoS display is used to generate different linear phases on the Fourier spectrum of an object, leading to different displacements of the object image sampled by CCD camera. By means of the proper combination of the different shifted images, a super-resolved image of the object is obtained. In addition, an inverse filtering process is applied as well, enabling to decrease, to a certain extent, the blurring effect introduced due to the intensity average performed inside the pixels area. Experimental results are provided in this work, showing the significant improvement in resolution of the images obtained with the proposed technique.

REFERENCES

- [1] W. Lukosz, "Optical systems with resolving powers exceeding the classical limits II," *J. Opt. Soc. Am* 57, 932-941 (1967).
- [2] Z. Zalevsky and D. Mendlovic, *Optical Super Resolution*, (Springer, 2002).
- [3] A. Shemer, D. Mendlovic, Z. Zalevsky, J. Garcia, and P. G. Martinez, "Super resolving optical system with time multiplexing and computer decoding," *Appl. Opt.* 38, 7245–7251(1999).
- [4] Z. Zalevsky, J. Solomon, and D. Mendlovic, "Geometrical super-resolution using code division multiplexing," *Appl. Opt.* 42,32–40 (2005).
- [5] A. Borkowski, Z. Zalevsky and B. Javidi, "Geometrical superresolved imaging using non-periodic spatial masking", *J. Opt. Soc. Am. A* 26, 589 (2009).
- [6] M. Sohail and A.A. Mudassar, "Geometric super-resolution by using an optical mask," *Appl. Opt.* 49, 3000–3005 (2010).
- [7] A. Borkowski, Z. Zalevsky, E. Marom, B. Javidi, "Enhanced geometrical super-resolved imaging with moving binary random mask", *J. Opt. Soc. Am. A / Vol. 28, No. 4 / April 2011*.
- [8] M. Sohail, A.A. Mudassar, "Geometric super-resolution using an optical rectangular mask", *Optical Engineering, Volume 51 (1) SPIE – Jan 1, 2012*.
- [9] Z. Zalevsky, D. Mendlovic and E. Marom, "Special sensor masking for exceeding system geometrical resolving power," *Opt. Eng.* 39, 1936–1942 (2000).
- [10] A. Ashok and M.A. Neifeld, "Pseudorandom phase masks for superresolution imaging from

subpixelshifting," *Appl. Opt.* 46, 2256–2268 (2007).

[11] I. U.Haq, A.A. Mudassar, "Geometric superresolution of a CCD pixel", *Opt. Lett/ Vol. 35, No. 16 / August 15, 2010*.

[12] J.W. Goodman, *Introduction to Fourier Optics* (McGraw-Hill, 1996).

[13] M. Ben-Ezra, A. Zometand S. K. Nayar, "Video super-resolution using controlled subpixel detector shifts", *IEEE Trans. Pattern Anal. Mach. Intell.* 27(6), 977–987 (2005).

[14] K. Yu, N. Park, D. Lee and O. Solgaard, "Superresolution digital image enhancement by subpixel imagetranslation with a scanning micromirror," *IEEE J. Sel. Top. Quantum Electron.* 13(2), 304–311 (2007).

[15] H.C. Lan, M.L. Wu and E.M. Yeatman, "Non-mechanical sub-pixel image shifter for acquiring super-resolution digital images", *Opt. Exp.* 17(25), 22992-23002 (2009).

[16] J. C. Russ, *The image processing Handbook*, (CRC Press, Taylor & Francis Group, 2011).